On-Line Supporting Information

High-Throughput Ultrasensitive Characterization of Chemical, Structural and Plasmonic Properties of EBL-Fabricated Single Silver Nanoparticles

Tao Huang,[a¥] Wei Cao,[b¥] Hani E. Elsayed-Ali,[b,c*] and Xiao-Hong Nancy Xu,[a*]

Departments of Chemistry and Biochemistry,[a] Applied Research Center,[b] and Electrical and Computer Engineering,[c] Old Dominion University, Norfolk, VA 23529

The On-Line Supporting Information (SI) includes:

(A) Materials and Methods

(B) Four Figures:

Fig. S1: Study of blue-shifts of LSPR spectra of single square-shaped NPs over their 12-week exposure to ambient conditions.

Fig. S2: Characterization of blue-shifts of LSPR spectra of single triangular NPs over their 12-week exposure to ambient conditions.

Fig. S3: Enlarged and high-resolution images of Fig. 4A in main text.

Fig. S4: Enlarged and high-resolution images of Fig. 5A in main text.

(C) References

¥ Both authors contribute equally to this work.
* To whom correspondence should be addressed: Email: xhxu@odu.edu; Tel/fax: (757) 683-5698; Email: helsayed@odu.edu; Tel: (757) 269-5645; Fax: (757) 269-5644

Materials and Methods

Fabrication of Single Ag NP Arrays Using EBL

Single Ag NP arrays (25x25) were fabricated on microscopic glass slides coated with indium tin oxide (30-nm thickness) using EBL apparatus (ELPHY Quantum, Raith, Ronkonkoma) coupled with SEM (JSM-6060LV, JEOL). The slides (substrates) were spin-coated with polymethylmethacrylate (PMMA) positive photoresist, followed by EB exposure at 30 kV. The samples were developed in a developer with a ratio of methyl-isobutyl-ketone (MIBK) to isopropanol (IPA) at 1:3 for 30 s, and rinsed with IPA for 30 s to stop the development. The Ag thin films were deposited on PMMA-patterned slides using a standard thermal evaporation process at the deposition rate of ~0.5 Å/s to achieve desired thickness. The standard lift-off process was carried out to achieve the NPs with desired sizes, shapes and configured arrays. The inter-NP distances among neighboring individual NPs on the array were controlled at the minimal of 3.2-μm apart to eliminate potential dipole coupling of LSPR of individual NPs.

Characterization of Chemical, Structural and Plasmonic Properties of Single Ag NPs

The samples (microscope slides with EBL-fabricated single Ag NP arrays) were wrapped with Al-foil and placed under ambient conditions in the lab (air-conditioned dark room; 45-55% relative humidity; atmosphere; 25^0C) over 12 weeks. Individual NPs on the arrays were characterized in parallel using SEM/EDS, AFM (Dimension 3100, Veeco), and DFOMS.

Four corners of each array were marked with four different symbols using EBL, which can be easily recognized by all three imaging scopes (SEM, AFM, and DFOMS). This simple approach enables us to locate any given single NPs in the array, identify and characterize the same NP in each array using SEM, AFM and DFOMS to better understand chemical and

morphological dependent LSPR spectra of single NPs over the duration of their exposure to the ambient conditions.

LSPR images and spectra of single NPs in the array were acquired simultaneously as the following. The deionized (DI) water was sandwiched between the nano-array microscopic slide and microscopic coverslip, which was then sealed to create a microchamber as the Xu group described previously.[1-3] LSPR images and spectra of single Ag NPs on each entire array on the slide immersed under the DI water were acquired individually and simultaneously in 5-100 milliseconds using DFOMS. Design and construction of DFOMS for characterization of single NPs were fully presented in our previous studies.[1-6] In this study, the dark-field optical microscope is equipped with a dark-field condenser (oil, 1.43-1.20), a microscope illuminator (Halogen lamp, 100 W), a 100x objective (Plan fluor 100x, N.A. 0.5-1.3), and Multispectral Imaging System (MSIS) (N-MSI-VIS-FLEX, CRI, CCD camera equipped with liquid-crystal tunable filter, LCTF).[7] The illumination power on the focal plane of dark field (sample stage) was measured as (0.070 ± 0.001) Watt using a power meter (Melles Griot)

References

1. X.-H. N. Xu, J. Chen, R. B. Jeffers and S. V. Kyriacou, *Nano Lett.*, 2002, **2**, 175-182.
2. Y. Song, P. D. Nallathamby, T. Huang, H. Elsayled-Ali and X.-H. N. Xu, *J. Phys. Chem. C.*, 2010, **114**, 74-81.
3. T. Huang and X.-H. N. Xu, *Nanoscale*, 2011, **3**, 3567-3572.
4. P. D. Nallathamby, T. Huang and X.-H. N. Xu, *Nanoscale*, 2010, **2**, 1715-1722.
5. P. D. Nallathamby, K. J. Lee, T. Desai and X.-H. N. Xu, *Biochemistry*, 2010, **49**, 5942-5953.
6. X.-H. N. Xu, W. J. Brownlow, S. V. Kyriacou, Q. Wan and J. J. Viola, *Biochemistry*, 2004, **43**, 10400-10413.
7. S. C. Gebhart, R. C. Thompson and A. Mahadevan-Jansen, *Appl. Opt.*, 2007, **46**, 1896-1910.

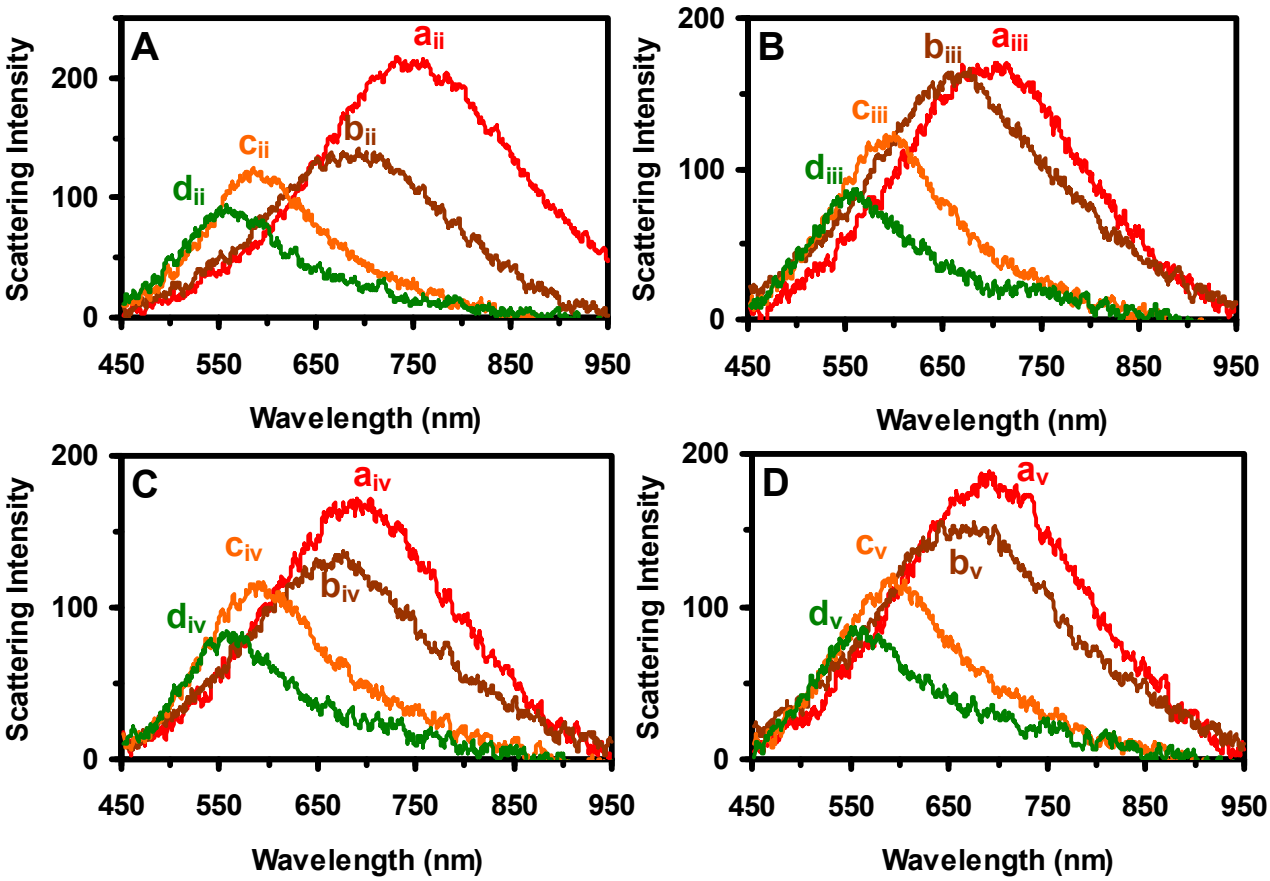

Figure S1: Study of the blue-shifts of LSPR spectra of single square-shaped NPs on the arrays marked as NP **(A)** (ii), **(B)** (iii), **(C)** (iv), and **(D)** (v) in Fig. 4B over their exposure to the atmosphere for **(a)** 0, **(b)** 1, **(c)** 4 and **(d)** 12 weeks. The λ_{max} (FWHM) of LSPR spectra of single NPs are: (a_{ii}) 733 (245), (b_{ii}) 666 (185), (c_{ii}) 586 (162), and (d_{ii}) 561 (126) nm for **(A)**; (a_{iii}) 738 (202), (b_{iii}) 659 (187), (c_{iii}) 600 (169), and (d_{iii}) 560 (127) nm for **(B)**; (a_{iv}) 720 (214), (b_{iv}) 653 (179), (c_{iv}) 595 (161), and (d_{iv}) 558 (122) nm for **(C)**; and (a_{v}) 692 (207), (b_{v}) 641 (188), (c_{v}) 594 (163), and (d_{v}) 562 (125) nm for **(D)**.

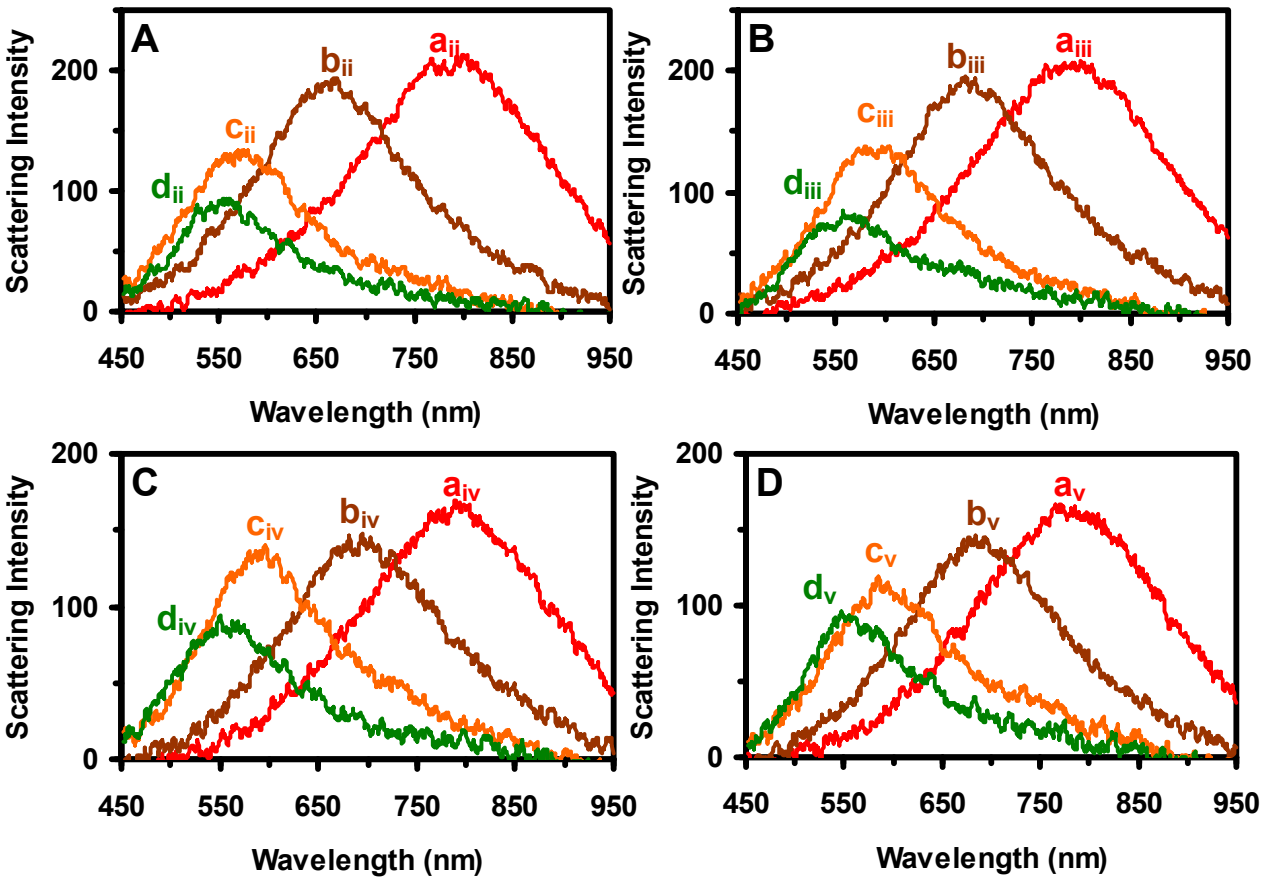

Figure S2: Study of the blue-shifts of LSPR spectra of single triangular NPs on the arrays labeled as NP **(A)** (ii), **(B)** (iii), **(C)** (iv), and **(D)** (v) in Fig. 5B over their exposure to the atmosphere for **(a)** 0, **(b)** 1, **(c)** 4 and **(d)** 12 weeks. The λ_{max} (FWHM) of LSPR spectra of single NPs are: (a_{ii}) 801 (263), (b_{ii}) 674 (218), (c_{ii}) 581 (169), and (d_{ii}) 561 (141) nm for **(A)**; (a_{iii}) 795 (258), (b_{iii}) 691 (215), (c_{iii}) 599 (183), and (d_{iii}) 557 (144) nm for (B); (a_{iv}) 793 (252), (b_{iv}) 701 (212), (c_{iv}) 598 (185), and (d_{iv}) 551 (143) nm for (C); (a_{v}) 774 (255), (b_{v}) 691 (188), (c_{v}) 593 (183), and (d_{v}) 548 (146) nm for (D).

Figure S3a

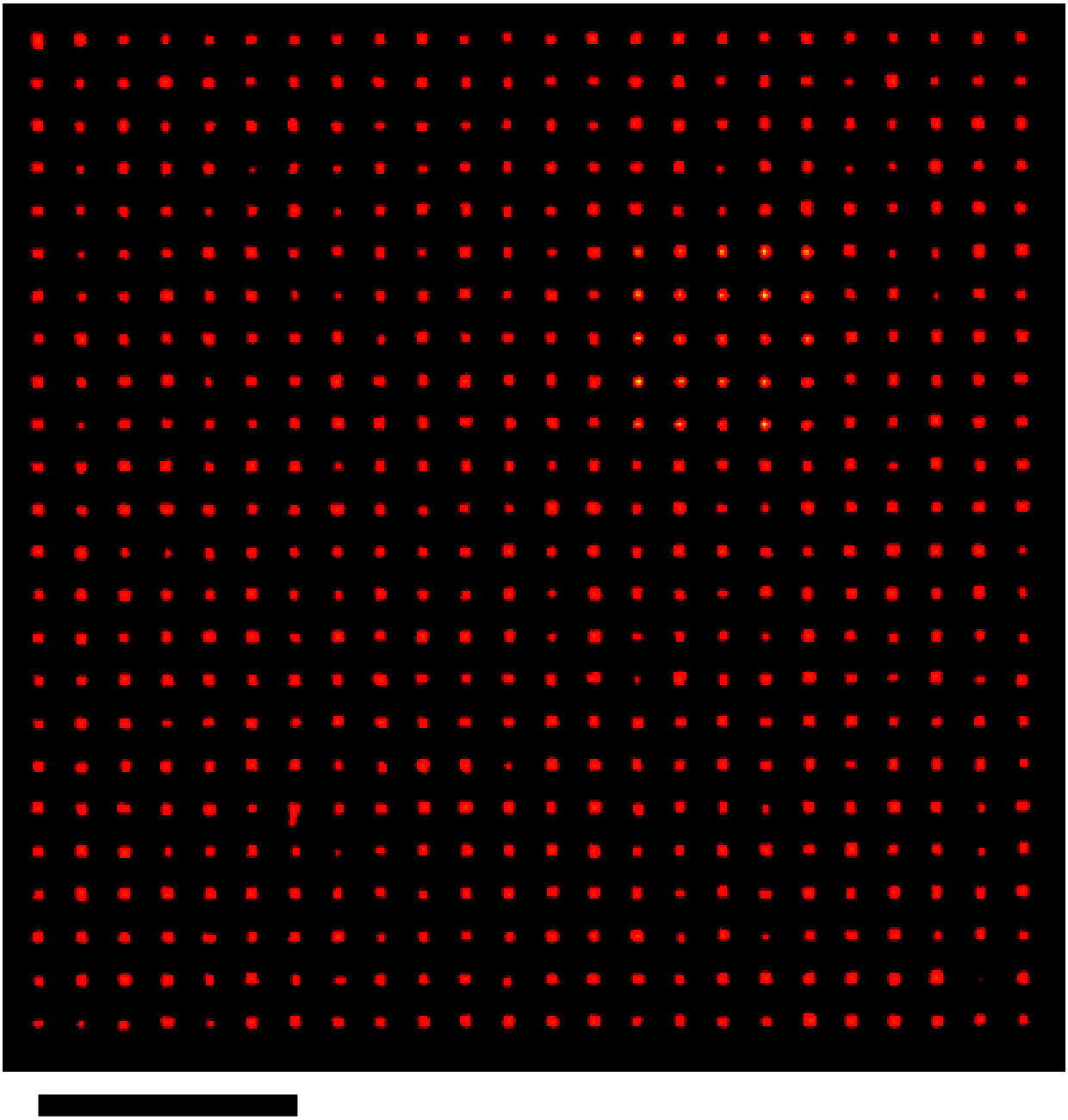

Figure S3b

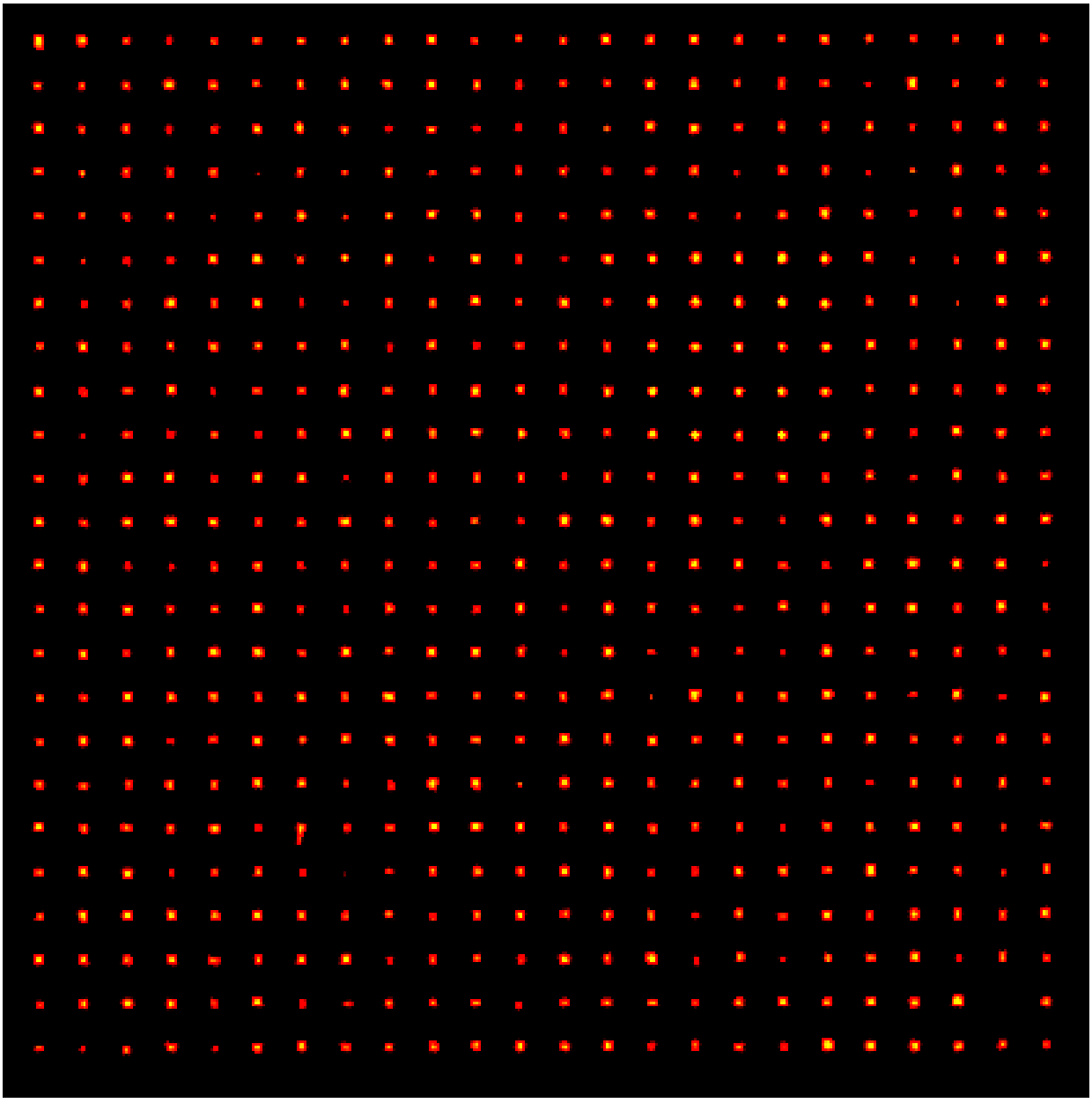

Figure S3c

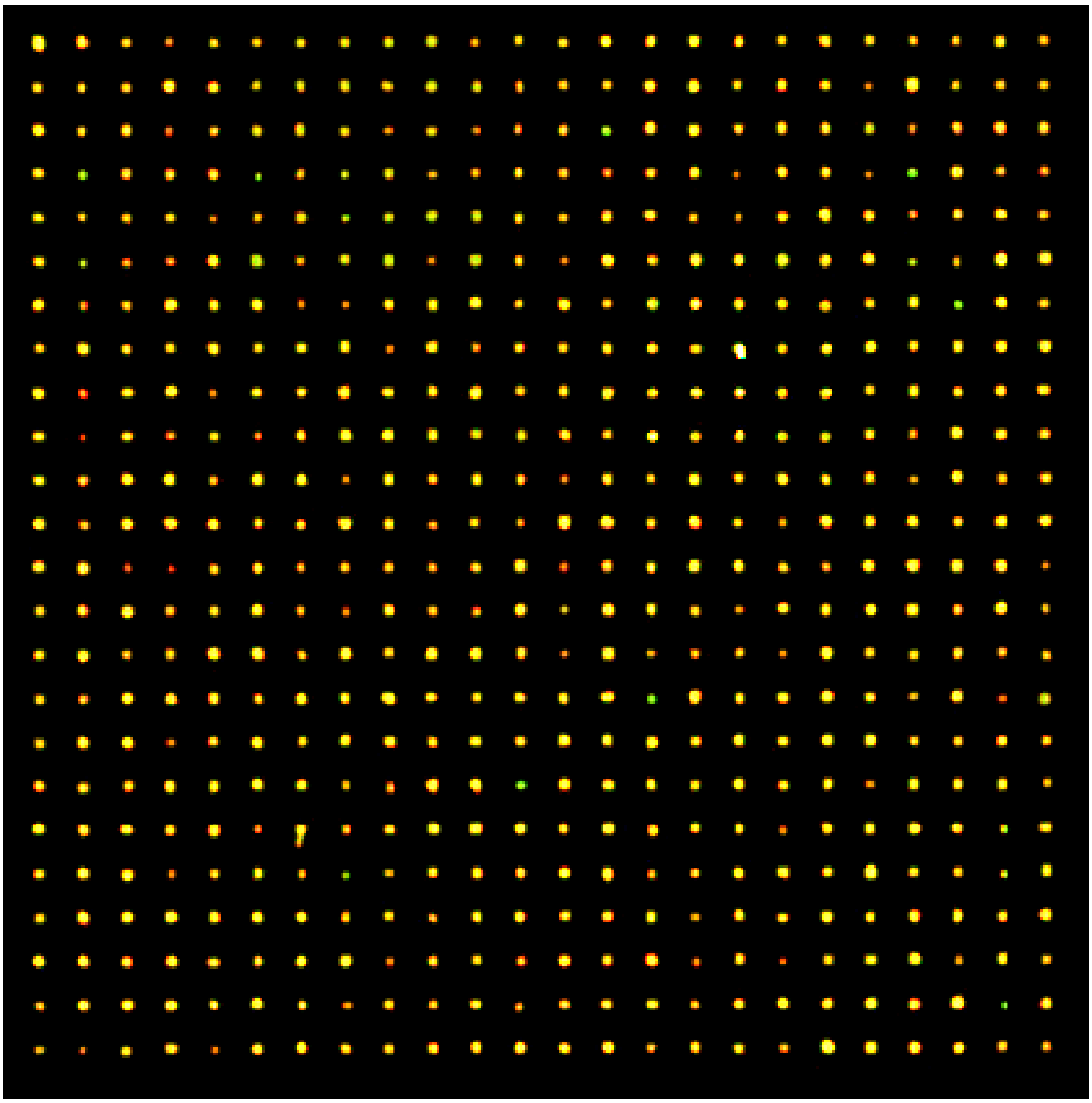

Figure S3d

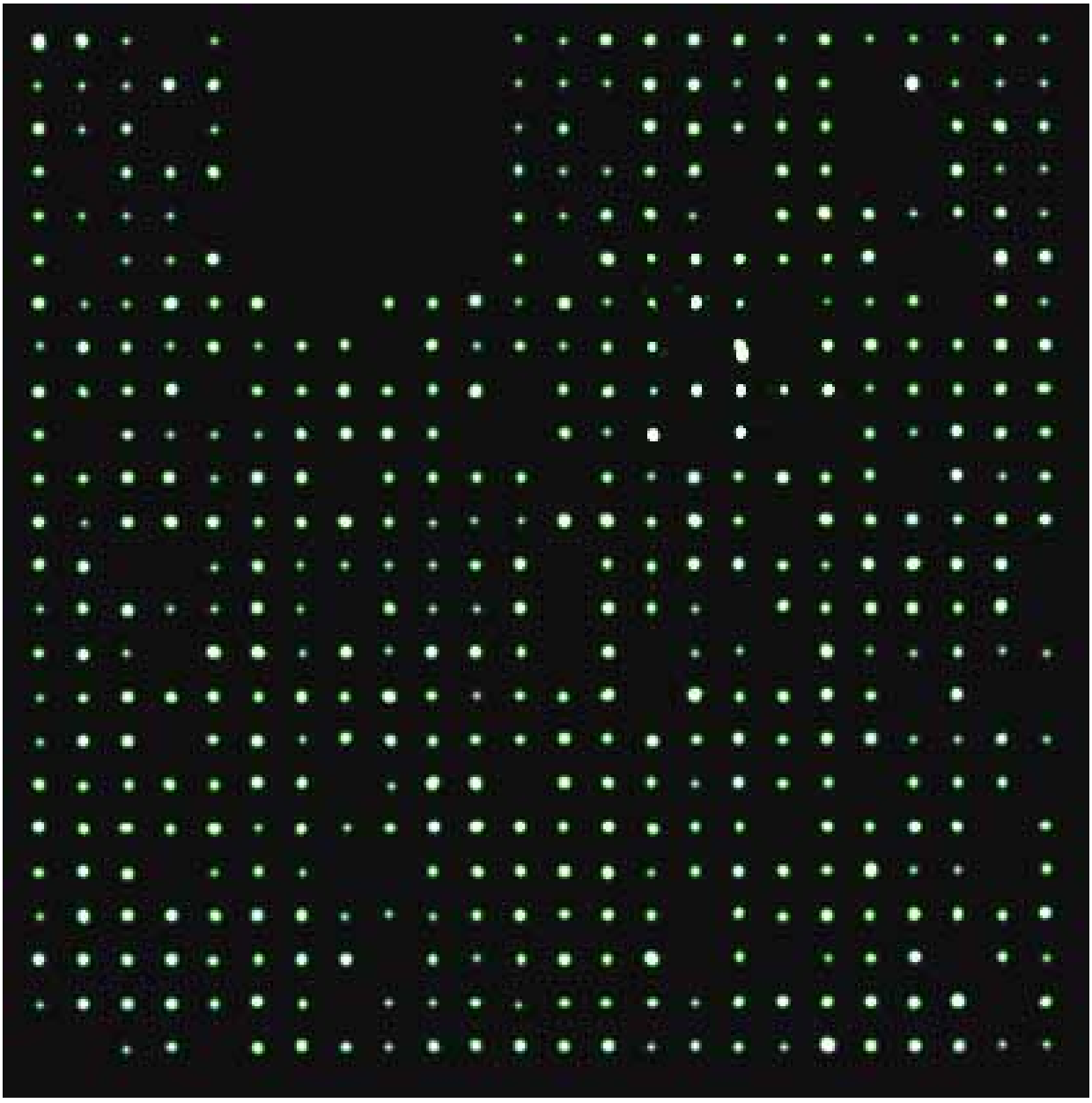

Figure S3: (a-d) Enlarged and high-resolution images of Figure 4A(a-d) in main text, respectively. Scale bars are 20 μm for all images.

Figure S4a

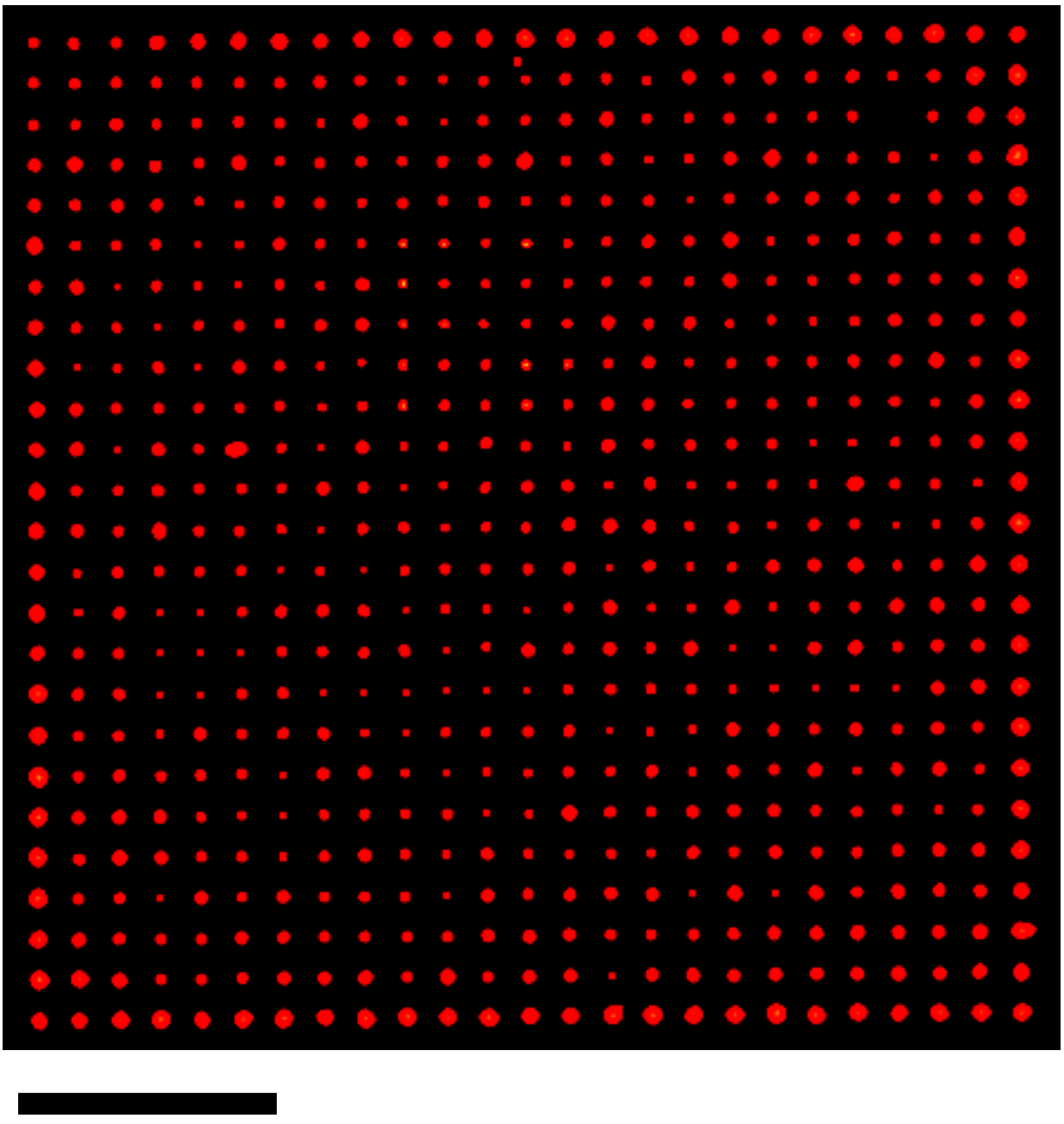

Figure S4b

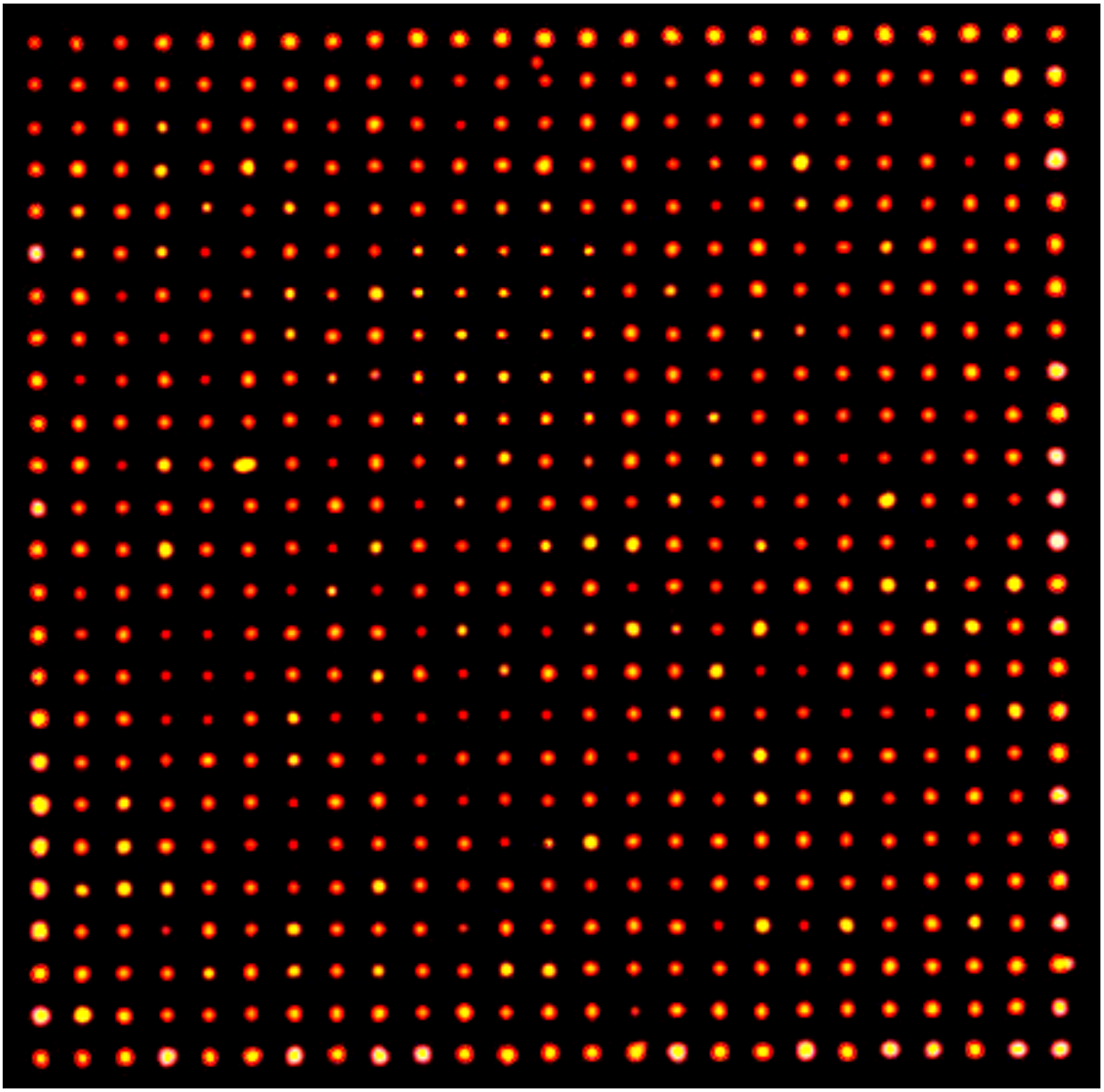

Figure S4c

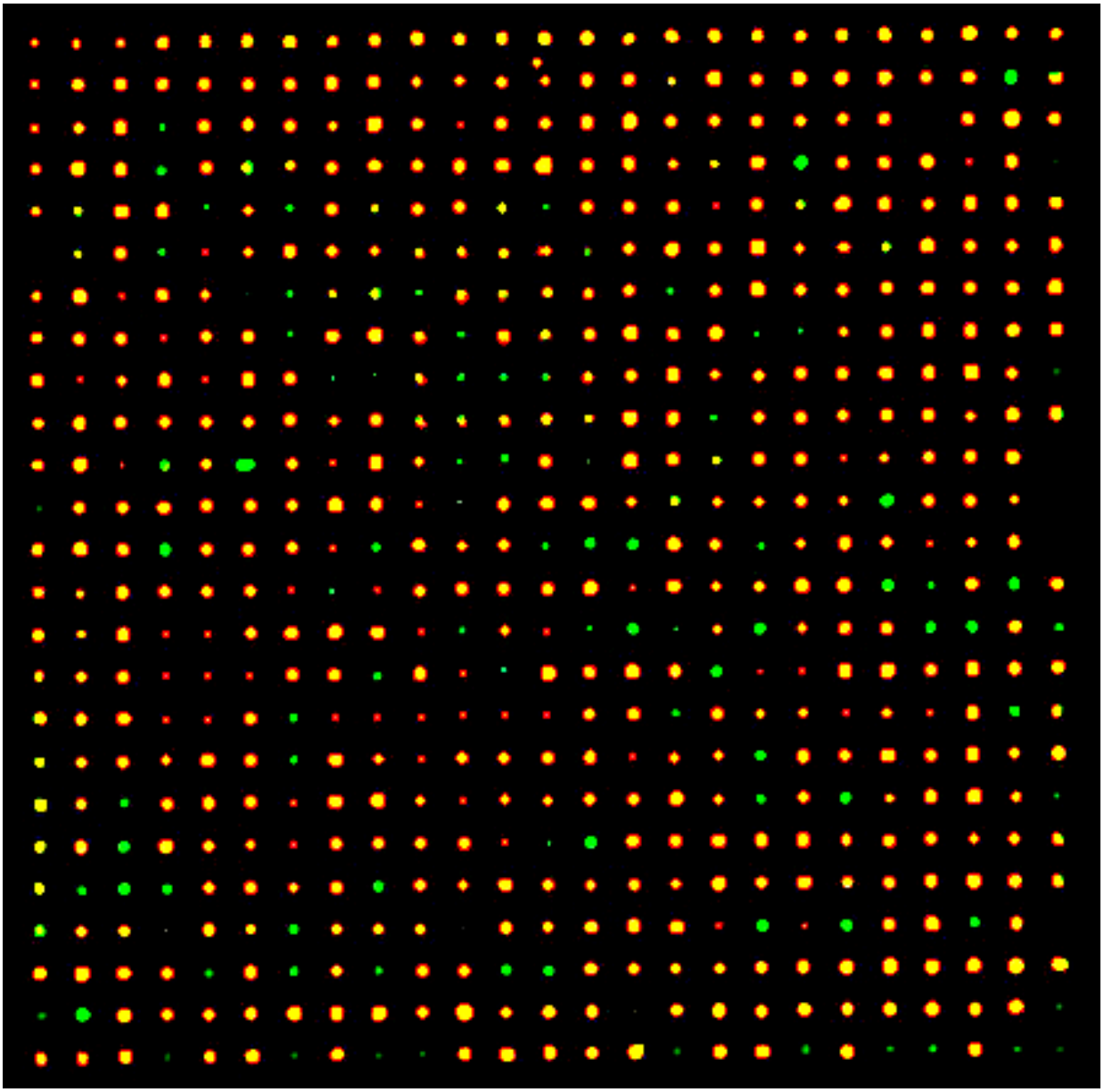

Figure S4d

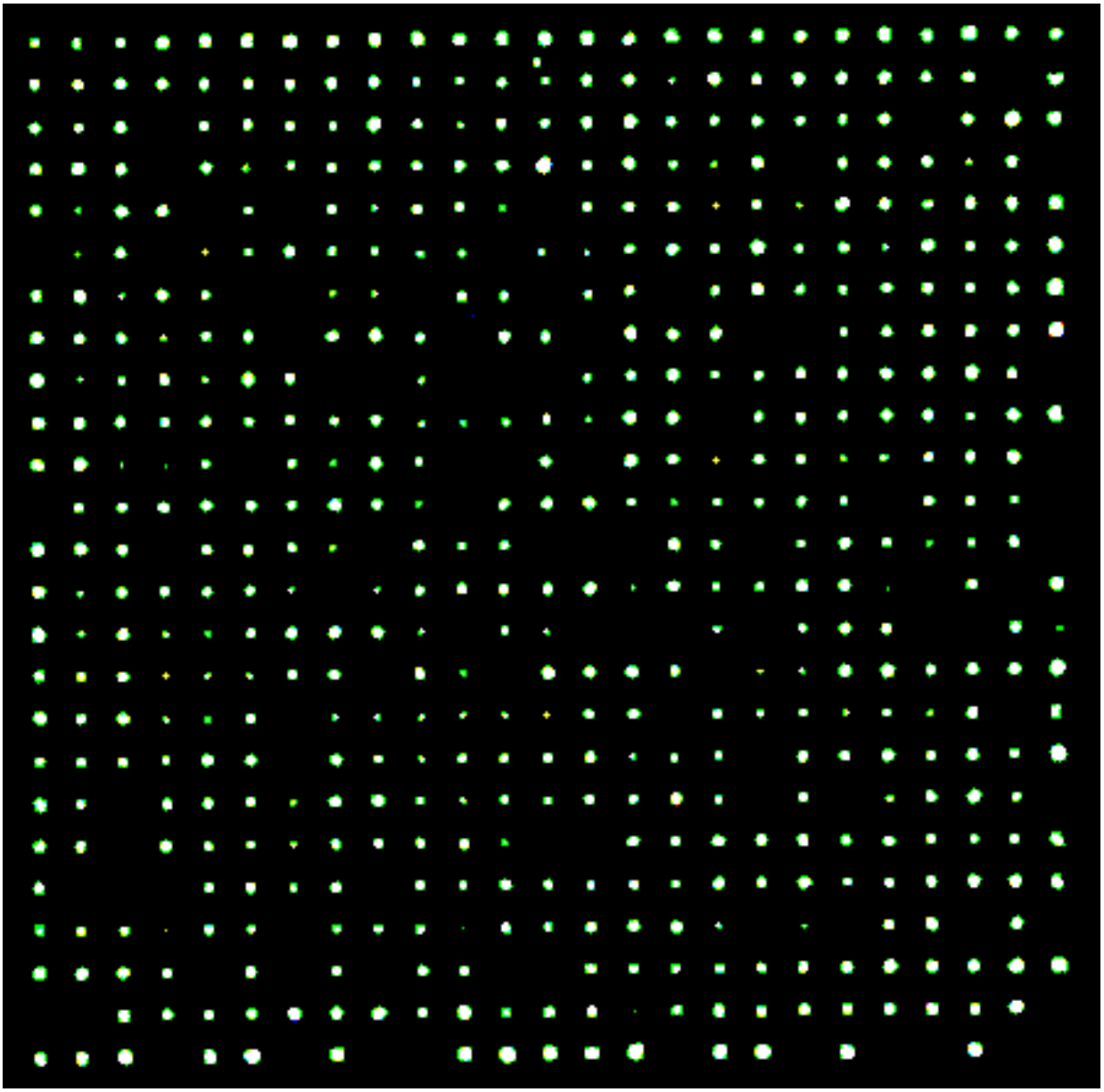

Figure S4: (a-d) Enlarged and high-resolution images of Figure 5A(a-d) in main text, respectively. Scale bars are 20 μm for all images.